

This document
Reproduced From
Best Available Copy

UNCLASSIFIED

AD. 4 4 3 1 5 2

DEFENSE DOCUMENTATION CENTER

FOR

SCIENTIFIC AND TECHNICAL INFORMATION

CAMERON STATION ALEXANDRIA, VIRGINIA



UNCLASSIFIED

This document
**Reproduced From
Best Available Copy**

NOTICE: When government or other drawings, specifications or other data are used for any purpose other than in connection with a definitely related government procurement operation, the U. S. Government thereby incurs no responsibility, nor any obligation whatsoever; and the fact that the Government may have formulated, furnished, or in any way supplied the said drawings, specifications, or other data is not to be regarded by implication or otherwise as in any manner licensing the holder or any other person or corporation, or conveying any rights or permission to manufacture, use or sell any patented invention that may in any way be related thereto.

APR 12 1963

REPORT 461

REPORT 461

ADVISORY GROUP FOR AERONAUTICAL RESEARCH AND DEVELOPMENT

64 RUE DE VARENNE, PARIS VII

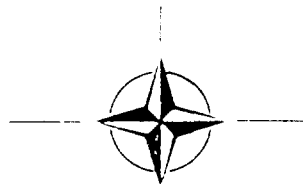
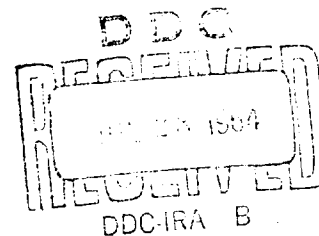
REPORT 461

**RECENT EXPERIMENTAL INVESTIGATIONS
ON THE SCATTERING OF SOUND BY
TURBULENCE**

by

DIETER W. SCHMIDT

APRIL 1963



NORTH ATLANTIC TREATY ORGANIZATION

This document
Reproduced From
Best Available Copy

443152

REPORT 461

NORTH ATLANTIC TREATY ORGANIZATION
ADVISORY GROUP FOR AERONAUTICAL RESEARCH AND DEVELOPMENT

RECENT EXPERIMENTAL INVESTIGATIONS
ON THE SCATTERING OF SOUND BY TURBULENCE

by

Dieter W. Schmidt

This Report is one in the Series 448-469 inclusive, presenting papers, with discussions, given at the AGARD Specialists' Meeting on 'The Mechanism of Noise Generation in Turbulent Flow' at the Training Center for Experimental Aerodynamics, Rhode-Saint Genèse, Belgium, 1-5 April 1963, sponsored by the AGARD Fluid Dynamics Panel

**Reproduced From
Best Available Copy**

SUMMARY

Experimental investigations of the scattering of sound by turbulence were performed in a wind tunnel. Recent theoretical predictions concerning the sound attenuation are well confirmed and partly extended by the measurements. In the range of the parameters which is of interest for practical applications the most important results obtained are the proportionality of the sound attenuation to the square of the sound frequency and to the square of the turbulent Mach number. A formula is derived from which the turbulent attenuation of directed sound (such as aircraft noise in the free atmosphere) can be calculated. A method for measuring large phase variations is described in preliminary form; it will be used to investigate the influence of turbulent scattering on the phase angle of the sound waves.

SOMMAIRE

Des recherches expérimentales sur la dispersion du son par turbulence ont été effectuées dans un tunnel aérodynamique. Les récentes prédictions théoriques concernant l'atténuation du son sont bien confirmées et partiellement élargies du fait des mesures obtenues. Dans la gamme des paramètres présentant de l'intérêt du point de vue des applications pratiques, les plus importants résultats obtenus sont la proportionnalité de l'atténuation du son au carré de la fréquence sonore et au carré du nombre de Mach turbulent. On en obtient une formule d'après laquelle il est possible de calculer l'atténuation turbulente du son dirigé (par exemple le bruit d'un avion dans l'atmosphère libre). On décrit sous forme préliminaire une méthode permettant de mesurer de grandes variations de phases; elle servira à étudier l'influence de la dispersion par turbulence sur l'angle de phase des ondes sonores.

534.26:532.517.4

1c5:3b2f

CONTENTS

	Page
SUMMARY	ii
SOMMAIRE	ii
LIST OF FIGURES	iv
NOTATION	vi
1. INTRODUCTION	1
2. EXPERIMENTAL PROCEDURE FOR ATTENUATION MEASUREMENTS	1
3. THEORETICAL PREDICTIONS	2
4. RESULTS OF MEASUREMENTS	3
5. SOME PRELIMINARY REMARKS ON THE MEASUREMENT OF PHASE ANGLE VARIATIONS	6
ACKNOWLEDGEMENT	7
REFERENCES	8
FIGURES	9
DISCUSSION	23
DISTRIBUTION	

LIST OF FIGURES

	Page
Fig.1 Schematic sketch of the scattering of sound by turbulence	9
Fig.2 Block diagram of the test set-up	10
Fig.3 Oscillograms showing transmitted and received sound pulses (upper and lower trace, respectively). First oscillogram obtained without flow, second and third ones with turbulent flow in the test duct (the same flow in both pictures)	11
Fig.4 Examples of oscillograms, each one showing one directly received sound pulse, followed by reflections, and the portion selected for measurement (upper and lower trace, respectively). First oscillogram obtained without flow, second and third ones with turbulent flow in the test duct (the same flow in both pictures)	12
Fig.5 Attenuation ΔI of sound vs. frequency of sound in the transition region between the asymptotic power laws $\Delta I \sim \nu^2$ and $\Delta I \sim \nu^5$	13
Fig.6 Attenuation ΔI of sound vs. dynamic pressure q of the main flow	14
Fig.7 Attenuation ΔI of sound vs. the product of the dynamic pressure q of the main flow and the square of the sound frequency ν	15
Fig.8 Same as Figure 7 (test conditions changed)	16
Fig.9 Same as Figure 7 (test conditions changed)	17
Fig.10 Graphic representation of Equation (9) for the estimation of the scattering of sound by turbulence in the atmosphere	18
Fig.11 Dependence of the turbulent sound attenuation ΔI on a predominant direction of the scattering vortices	18
Fig.12 Example of the regular amplitude modulation of ultrasound which has traversed the wake flow of a single bar. This pattern was obtained by superimposing three received sound pulses on the same picture	19
Fig.13 Multiple oscillogram showing the relationships in time between some voltages which participate in the generation of phase-measuring sawtooth pulses	19

		Page
Fig. 14	Double-beam oscillogram simultaneously showing phase- and amplitude-variations. It represents a time interval of 0.5 ms selected from within a received ultrasonic pulse in the case of laminar flow in the test duct (sound frequency: 129 kcps)	20
Fig. 15	Same as Figure 14, but in the case of weak turbulent flow in the test duct	20
Fig. 16	Same as Figure 14, but in the case of strong turbulent flow in the test duct	21
Fig. 17	Double-beam oscillogram simultaneously showing phase- and amplitude-variations. It represents a time interval of 3 ms selected from within a received ultrasonic pulse in the case of strong turbulent flow in the test duct (sound frequency: 300 kcps)	21

NOTATION

ν	frequency of sound
M'	Mach number of the turbulence $\left(= \frac{u'}{a_0} \right)$
u'	rms value of the turbulent fluctuation velocity $\left(= \sqrt{\left\langle \frac{1}{3} (\overline{u_x^2} + \overline{u_y^2} + \overline{u_z^2}) \right\rangle} \right)$
u_x, u_y, u_z	fluctuation velocities in x,y,z-direction, respectively
x, y, z	Cartesian space coordinates, x aligned with main flow
a_0	velocity of sound
s	length of the sound path in turbulent flow
L_n	lateral macroscale of the turbulence $\left(= \int_0^\infty \frac{\overline{u_x(y_1) \cdot u_x(y_1 + y)}}{\sqrt{\overline{u_x(y_1)^2}} \cdot \sqrt{\overline{u_x(y_1 + y)^2}}} dy \right)$
L_n	non-dimensional lateral macroscale of the turbulence $\left(= \frac{L_n}{\lambda} \right)$
λ	wavelength of the sound
E_0	energy flux of the incident sound beam
E_s	energy flux of the scattered sound
d	distance of the turbulence grid from the sound beam axis (measured along a streamline of the main flow)
I^{lam}	sound intensity in the case of laminar flow
I^{turb}	same as I^{lam} , but in the case of turbulent flow
ΔI	sound attenuation
θ	angle between the propagation direction of the incident sound waves and the axes of the scattering vortices in the case of extremely non-isotropic turbulence
q	dynamic pressure of the main flow
C_1, C_2	constants in Equation (8)

k_1, k_2	non-dimensional constants in equation (9)
α	angle between the propagation direction of the incident sound waves and the rods of the turbulence grid
h	total length of the sound path
D	diameter of the rods of the turbulence grid
m	mesh length of the turbulence grid
S_S	diameter of sound transmitter
S_E	diameter of sound receiver

RECENT EXPERIMENTAL INVESTIGATIONS ON THE SCATTERING OF SOUND BY TURBULENCE

Dieter W. Schmidt*

1. INTRODUCTION

The sound which is radiated from a region of turbulent flow is governed primarily by the mechanism generating it. In many cases, however, one has to account for the fact that the sound which is generated by a turbulent flow is also scattered by this flow before leaving the turbulent field. Hence, scattering may have an influence on the radiation pattern of jet noise, for instance. Furthermore, scattering by turbulence is important in the propagation of sound in the atmosphere or in tubes. In order to gain some basic understanding about the scattering of sound by turbulence, some experimental investigations were performed at the Max-Planck-Institut für Strömungsforschung in Göttingen¹ under well known and reproducible laboratory conditions. The results thus obtained were compared with the predictions given by theory.

The problem is governed by the following parameters of the flow field and the sound field:

1. the sound frequency ν ,
2. the Mach number of the turbulence $M' = \frac{u'}{a_0}$ (u' is the root-mean-square value of the turbulent fluctuation velocity, a_0 is the sound speed),
3. the length s of the sound path in the turbulent medium,
4. a characteristic length of the turbulence, e.g. the lateral macroscale L_n ,
5. the character of the turbulence with respect to homogeneity and isotropy.

From these parameters two non-dimensional numbers may be derived which will be of importance: the non-dimensional lateral macroscale ζ_n and the product $M' \cdot \zeta_n$. Here ζ_n represents the lateral macroscale L_n , made dimensionless by dividing by the wavelength λ of the sound waves $\left(\zeta_n = \frac{L_n}{\lambda} = \frac{L_n}{a_0} \cdot \nu \right)$.

2. EXPERIMENTAL PROCEDURE FOR ATTENUATION MEASUREMENTS

The principle of the scattering process and its measurement is shown in Figure 1: a beam of plane sound waves, the energy E_0 of which is known by measurement, runs through a region of turbulence. On passing through this turbulent region of length s it loses energy by scattering in the sideward directions, the energy flux E_0 thus

* Max-Planck-Institut für Strömungsforschung, Böttingerstrasse 6/8, 34 Göttingen, Germany

being reduced by E_s . The energy flux $E_0 - E_s$ of the emergent sound beam is measured. The attenuation can then be calculated from the measured values E_0 and $E_0 - E_s$.

A block diagram of the apparatus used is shown in Figure 2: the measurements were performed within the entrance region of a 30 x 12 cm test duct. In this region the natural turbulence of the flow is very weak, and the mean flow velocity is nearly constant over practically the entire cross-section. The flow is made turbulent by injecting a grid into the flow from an airtight cartridge. The flow region, which has constant turbulent mean value properties with respect to time and space along the sound beam, is traversed by a beam of high-frequency sound. The turbulent properties of the flow can be varied by changing the mean flow velocity, the geometry of the turbulence grid, and the distance d between the grid and the sound-beam axis. In order to avoid disturbances of the measurements due to reflected sound waves, the sound is transmitted in short pulses which are subject to a suitable selection in time on the receiving line.

Some double beam oscillograms of the transmitted and the received sound pulses denoted in Figure 2 by U4 and U5, respectively, and of the portion U8 of the received sound signals selected for measurement, are shown in Figure 3: on the upper trace of each of the three pictures one sees the sound pulses which are transmitted into the flow (U4 in Fig. 2). The sound frequency in the case shown was 200 kcps. The second trace gives a picture of the received sound pulses (U5 in Fig. 2), on the first oscillogram in the case of no flow in the test duct. The pulse length used is adjusted so that the directly received pulse ends just before the first reflected pulse reaches the receiving microphone; the recurrence frequency of the pulses, which was 100 cps in the case shown by Figure 3, only needs to be low enough to ensure that all multiple-reflected pulses have decayed before the next direct pulse is received. The second and the third oscillograms show the same situation as in the first picture, but with turbulent flow in the test duct. In this case the received sound pulses are modulated irregularly, and the mean amplitude is reduced by turbulent scattering.

Figure 4 shows one received sound pulse which is now present on the upper trace with a time base extended fourfold. In the first picture no flow is present, whereas in the two following pictures the flow is turbulent. The lower trace shows the portion of the received sound which is selected for measurement (U8 in the block diagram); it is free of reflected sound and of transient effects.

Two values were measured during each test run: the intensity I^{lam} of the received sound in the case of laminar flow (that is without scattering) and the corresponding value I^{turb} in the case of turbulent flow (that is with scattering). From these values the attenuation is obtained by applying the formula

$$\Delta I = 10 \log \frac{I^{lam}}{I^{turb}}. \quad (1)$$

3. THEORETICAL PREDICTIONS

Theoretical predictions of the dependence of the attenuation given by Equation (1)

on the parameters listed above were given, among others, by Lighthill², Kraichnan³, and by Müller and Matschat⁴. The following formulae for the attenuation ΔI which are valid for not too large values of $M' \cdot f_n$ were derived by Müller and Matschat:

$$\Delta I \sim \frac{L_n^4}{a_0^5} s \cdot M'^2 \cdot \nu^5 = \frac{s}{L_n} M'^2 \cdot f_n^5 \quad \text{for } f_n \ll 1 \quad (2)$$

$$\Delta I \sim \frac{L_n}{a_0^2} s \cdot M'^2 \cdot \nu^2 = \frac{s}{L_n} M'^2 \cdot f_n^2 \quad \text{for } f_n \gg 1 \quad (3)$$

for isotropic turbulence and

$$\Delta I \sim \sin^4 \theta (\sin^4 \theta + 4 \cos^4 \theta) \frac{L_n^4}{a_0^5} s \cdot M'^2 \cdot \nu^5 \quad (3)$$

$$\sin^4 \theta (\sin^4 \theta + 4 \cos^4 \theta) \frac{s}{L_n} M'^2 \cdot f_n^5 \quad \text{for } f_n \ll 1 \quad (4)$$

$$\Delta I \sim \sin^2 \theta \frac{L_n}{a_0^2} s \cdot M'^2 \cdot \nu^2$$

$$\sin^2 \theta \frac{s}{L_n} M'^2 \cdot f_n^2 \quad \text{for } f_n \gg 1 \quad (5)$$

for extremely non-isotropic turbulence, i.e. turbulence which is represented by a statistical superposition of vortices with parallel axes. In the latter case one has the same formulae as for isotropic turbulence, except for a θ -dependent factor, where θ is the angle between the direction of sound propagation and the direction of the axes of the scattering vortices. It is to be noted that, in all four limiting cases, ΔI is proportional to the length s of the sound path in the turbulent flow and to the square of the turbulent Mach number M' . However, the dependence on the sound frequency ν follows two different laws: a ν^5 -law for low values of f_n and a ν^2 -law for high f_n -values. The turbulence in the experiments reported here had properties lying between isotropy and extreme non-isotropy.

4. RESULTS OF MEASUREMENTS

In Figures 5 to 9 some results of attenuation measurements are plotted which were obtained by using several turbulence grids of different mesh lengths and rod diameters and at selected distances behind the grid.

From the data plotted in Figure 5 the dependence of the sound attenuation on the sound frequency is seen at two different conditions of turbulence, namely at two

different velocities of the main flow. The grid arrangement was the same for all measurements. Apart from a deviation at very high values of ν in the case of the higher main flow velocity, the explanation for which will become evident later, these measurements confirm the ν^2 -law at high sound frequencies. In the region of lower frequencies, however, ΔI increases with ν according to a higher power law. This change in the ascent corresponds to the region of transition between the asymptotic ν^2 -law and the asymptotic ν^5 -law which were predicted theoretically.

The next figure (Fig. 6) shows a series of measurements in which only the dynamic pressure q of the main flow was varied. As can be seen, ΔI increases linearly with q over a wide range of q . Since q can be assumed to be proportional to the Mach number M' of the turbulence behind a grid, this result confirms the proportionality of ΔI to M'^2 which was also predicted theoretically.

The results of measurements which are presented in Figures 7 to 9 were obtained by variation of the dynamic head q of the main flow as well as of the sound frequency ν . In all cases $M' \cdot f_n$ was greater than one. Then one has

$$(M' \cdot f_n)^2 \sim q \cdot \nu^2 \quad (6)$$

and hence, Formula (3) may be rewritten

$$\Delta I \sim \frac{s}{l_n} \cdot q \cdot \nu^2 \quad (7)$$

The data presented in Figure 7 correspond to low values of $M' \cdot f_n$ and are quite well represented by the relation $\Delta I \sim q \cdot \nu^2$ over the entire range of $q \cdot \nu^2$ -values covered by the measurements, thus again confirming the theoretical predictions.

The results presented in Figure 8 were obtained by use of a grid containing much thicker rods and, therefore, lead to higher values of $M' \cdot f_n$. At the lower $q \cdot \nu^2$ -values, which correspond to lower $M' \cdot f_n$ -values, the attenuation ΔI increases linearly with $q \cdot \nu^2$ as before. At higher values of $q \cdot \nu^2$, corresponding to higher $M' \cdot f_n$ -values, the quantity ΔI shows a slower increase than proportionality to $q \cdot \nu^2$; instead it follows a curve represented by the equation

$$\Delta I = C_1 \cdot \frac{C_2 \cdot q \cdot \nu^2}{1 + C_2 \cdot q \cdot \nu^2} \quad (8)$$

with properly chosen values of C_1 and C_2 . The straight line is the asymptote of the curve. This behaviour is even more marked in Figure 9. The only difference between the data presented in this Figure and those presented in the foregoing one is that the distance between the turbulence grid and the sound beam axis was reduced from 20 to 5 cm. By this means the product $M' \cdot f_n$ was further increased, as could be seen from separate measurements. Again the measurements proved to be well represented by Equation (8) with suitable values of C_1 and C_2 .

Combining the results discussed above (and some additional experimental data which will not be elaborated here in detail) one may derive the following non-dimensional formula:

$$\Delta I \frac{L_n}{s} = k_1 \frac{\left(\frac{u'}{a_0} \cdot \frac{L_n}{a_0} \right)^2}{1 + k_2 \left(\frac{u'}{a_0} \cdot \frac{L_n}{a_0} \right)^2} \quad (9)$$

It may be noted here that the term within the parentheses is equal to the product $M' \frac{L_n}{a_0}$. This formula, which was derived from the experimental results, extends the theoretical result which was derived for small $M' \frac{L_n}{a_0}$ -values only.

The constant k_1 proved to be dependent, to a certain degree, on the proportion between the diameter of the receiving microphone and the wavelength of the sound. The values $k_1 = 180$ and $k_2 = 8$, which were introduced for the graph given in Figure 10, were found to be valid for conditions which approximately correspond to the propagation of directed sound from airplanes in the free atmosphere. To get the order of magnitude of the scattering in the atmosphere under mean-weather-conditions, one has to estimate L_n and u' . As an example, according to measurements of Frankenberger⁵, one may take $L_n \approx 10$ m and $u' \approx 0.2$ m.s⁻¹. Under these assumptions the denominator of Equation (9) can be put equal to 1 up to frequencies of about 10 kcps, and one obtains simple proportionality of $\frac{\Delta I}{s}$ to ν^2 . The resulting order of magnitude is the same as was found by direct measurements of the attenuation of air-to-ground aircraft sound by Parkin and Scholes⁶.

Some further experiments were performed concerning the dependence of the attenuation ΔI on a predominant direction of the scattering vortices. For this purpose the test duct with rectangular cross-section was replaced by a tube with circular cross-section, and the turbulence grid was put into the test duct through the inlet nozzle. By rotating the grid (which, as before, consisted of parallel circular rods) about the tunnel axis the predominant direction of the axes of the scattering vortices could be varied continuously from 0° to 90° with respect to the sound beam axis. The results of measurements are shown in Figure 11. Here θ' is the angle between the rods of the turbulence grid and the direction of wave propagation. The sound attenuation increases monotonically with θ' running from 0° to 90°. The angle θ' can be identified with θ in the relation $\Delta I \sim \sin^2 \theta$ which was predicted theoretically for extremely non-isotropic turbulence (see Equation (5)). Hence, a qualitative agreement between the experiments and the theory can be inferred. Of course, ΔI cannot vanish at $\theta' = 0^\circ$ experimentally, since vortices are also present in the path of the sound waves with axis directions differing from those of the rods.

Some experiments on the scattering of sound which traverses the wake flow of a single circular rod may also be mentioned here. As is known from hot-wire measurements (see e.g. Roshko⁷), vortices with two distinct frequencies appear in such a wake flow not too far behind the rod. These frequencies are equal to the shedding frequency of the von Kármán vortices measured over either a single row, or the combined rows of vortices. In our experiments a marked regular modulation of the received sound amplitude by exactly the same frequencies was observed (see the oscillogram presented in Figure 12). This pattern was obtained by superimposing three received sound pulses on the same picture. One observes that during each pulse

interval four vortices have passed through the sound path in quite regularly spaced time intervals.

5. SOME PRELIMINARY REMARKS ON THE MEASUREMENT OF PHASE ANGLE VARIATIONS

The investigations reported here have, until now, been related to scattering influences on the amplitude of sound waves which run through turbulent flow. Further investigations were initiated to study the influence of turbulent scattering on the phase angle of the received sound. For this purpose a new method of measurement is just being developed which permits the measurement and registration of phase fluctuations of the sound.

In this method, the phase fluctuations are transferred linearly to amplitude fluctuations of sawtooth pulses. Thus the well known methods of statistical pulse height analysis can be applied. The operation of this measurement technique may shortly be described with the aid of Figure 13. This picture is a multiple oscillogram showing the relationships in time between some voltages which participate in the generation of the sawtooth pulses. The first trace corresponds to the constant frequency sine waves which are transmitted into the flow. The second trace shows the output of a square wave generator which is synchronized by the transmitted sound waves. Each negative voltage jump determines the exact instant at which the transmitted waves reach a certain phase angle. The third trace indicates some oscillations of the received sound. Each zero of the voltage with positive ascent starts a positive-going linear sawtooth as often as the sawtooth generator is ready to be triggered. Such a sawtooth pulse which is seen in the fourth trace is cut off by the next following negative jump of the square wave in the second trace. Hence, its height is proportional to the phase difference between a certain constant phase of the transmitted sound wave and zero phase of the received one. The last trace shows a pulse train which, for a certain time, blocks the mechanism by which sawtooth pulses are triggered. This time is needed for the completion of a sawtooth already in progress, for the retrace, and for the full recovery of the circuit. Thus, in the example shown, only each second cycle of sound waves is used to initiate a phase-measuring pulse.

As an example of the application of this method of phase angle measurement, some double-beam oscillograms may be presented which simultaneously show the phase- and amplitude-variations of the received sound. Figure 14 is such a picture of a sound pulse which has traversed only laminar flow. On the upper trace one sees the sawtooth pulses, the height of which is a measure of the phase angle of the received sound waves. The lower trace is a direct picture of the received sound pressure. In this laminar case one has no scattering and, hence, the phase and amplitude are constant. The pulse height shown in the picture corresponds to about 280° .

The next picture (Fig. 15) was taken with weak turbulent flow in the test duct. Due to scattering, the received sound fluctuates in phase and amplitude. The picture shown in Figure 16 corresponds to strong turbulence. In this case, phase angles exceeding 360° or even multiples of it may occur. To understand what then happens the simple case may be considered that the phase angle increases (decreases) monotonically through the specific phase angle of 360° . For phase angles up (down)

to 360° the height of the sawtooth pulses will then also increase (decrease) monotonically since it depends linearly on the phase angle. However, at the instant the phase angle passes through 360° the pulse height reaches a maximum (zero) value and then jumps back to a zero (maximum) value (a jump of this kind is seen in Figure 16). In order to obtain the true absolute value of the phase angle for the time following this jump, one then has to add (subtract) 360° to the value of the phase angle which one would ordinarily deduce by simply measuring the height of the sawtooth pulses. In the more complicated case where several jumps (possibly in both positive and negative directions) occur, the result correspondingly must be modified by counting the algebraic number of these jumps and then adding the corresponding multiples of 360° to the measured pulse height. This is accomplished automatically at each instant by applying electronic counting methods. The reference value for all phase angle measurements within a special received sound pulse is given by the initial phase angle in this pulse. This initial value of the phase shift may vary from sound pulse to sound pulse and, hence, is determined additionally for each received pulse by measuring the time delay of its starting point with respect to the starting point of the corresponding transmitted sound pulse.

As an additional example, Figure 17 shows the variations in phase and amplitude within a received sound pulse for a longer time interval in the case of strong turbulent flow. As was described above, the maximum height of the sawtooth pulses which is present near the jump corresponds to a phase angle of 360° . As could be seen from many other oscillograms of this kind, a correlation exists between the minima of the received sound pressure and the steep slopes of the phase angle variations, both of which are due to strong turbulent scattering of the sound.

It is hoped that further understanding of the scattering mechanism will be gained with the help of the measuring method just described.

ACKNOWLEDGEMENT

This research was supported in part by the United States Air Force under Grant No. EOARD-61-5 and Grant No. AF-EOAR 63-56 and monitored by the European Office, Office of Aerospace Research.

REFERENCES

1. Schmidt, D. *Experimentelle Untersuchungen über die Streuung von Schall in turbulenter Strömung.* Mitt. MPI für Strömungsforschung und AVA Göttingen, Nr. 28, 1962.
2. Lighthill, M.J. *On the Energy Scattered from the Interaction of Turbulence with Sound or Shock Waves.* Proc. Cambr. Phil. Soc., Vol. 49, 1953, pp. 531-551.
3. Kraichnan, R.H. *The Scattering of Sound in a Turbulent Medium.* J. Acoust. Soc. Am., Vol. 25, 1953, pp. 1096-1104.
Errata: J. Acoust. Soc. Am., Vol. 28, 1956, p. 314.
4. Müller, E.A.
Matschat, K.R. *The Scattering of Sound by a Single Vortex and by Turbulence.* AFOSR TN 59-337, AD 213658, 1959.
5. Frankenberger, E. *Über den Vertikalaustausch.* Beitr. Phys. Atmos., Bd. 32, 1958, pp. 283-299.
6. Parkin, P.H.
Scholes, W.E. *Air-to-Ground Sound Propagation.* J. Acoust. Soc. Am., Vol. 26, 1954, pp. 1021-1023.
7. Roshko, A. *On the Development of Turbulent Wakes from Vortex Streets.* NACA Rep. No. 1191, 1954.

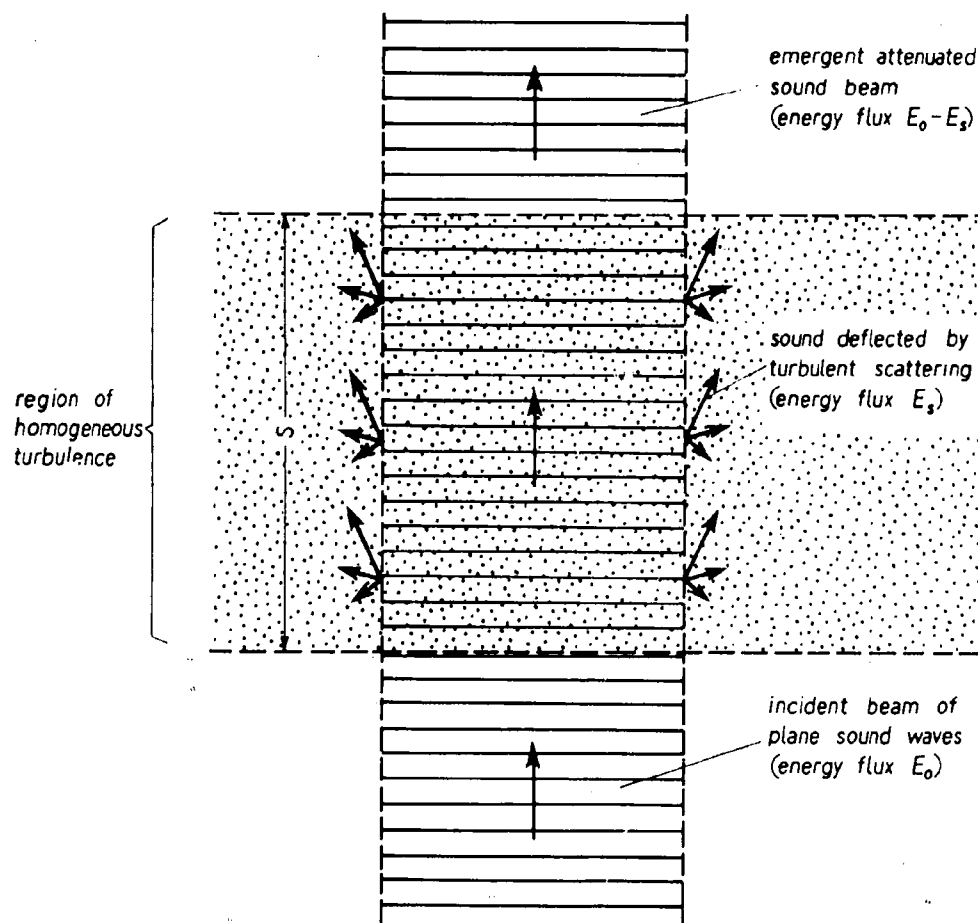


Fig. 1 Schematic sketch of the scattering of sound by turbulence

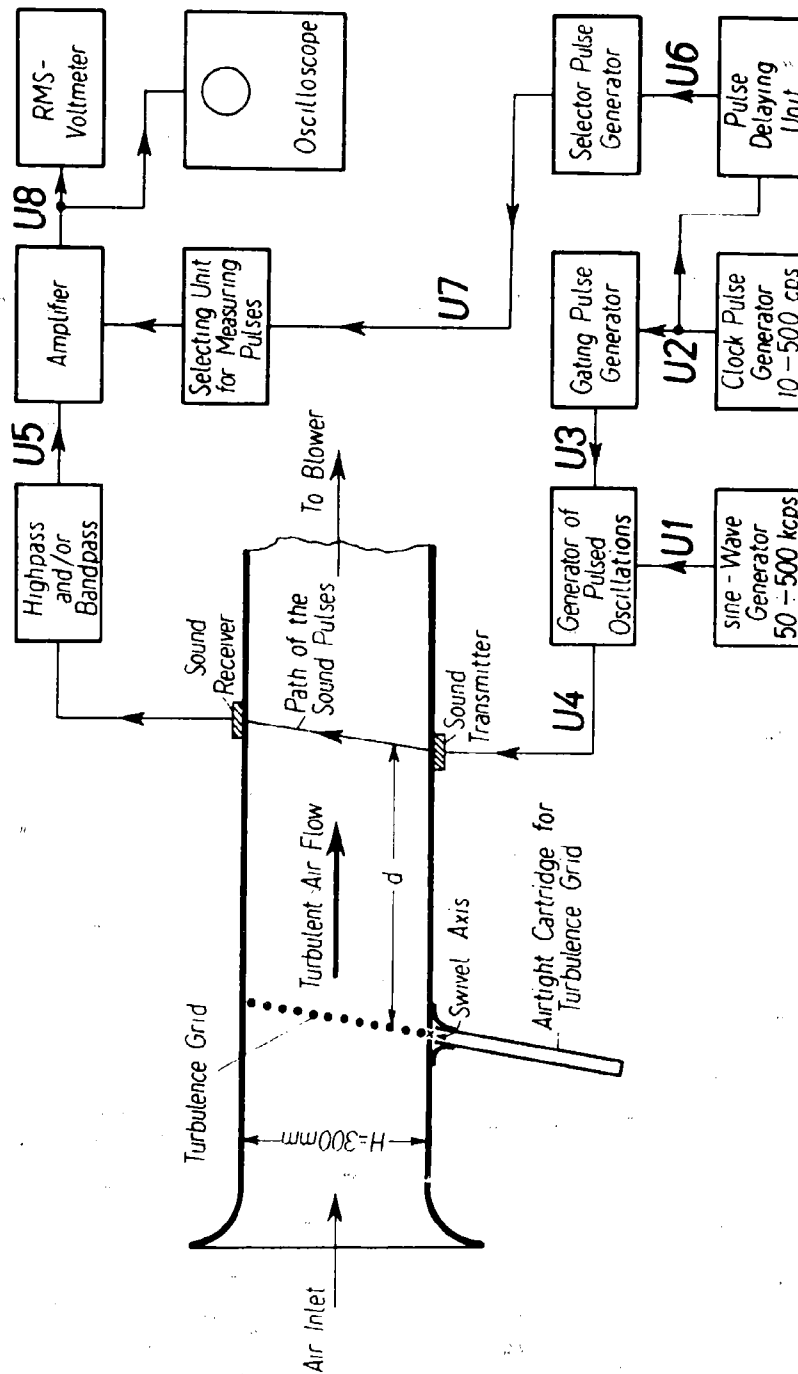


Fig. 2 Block diagram of the test set-up

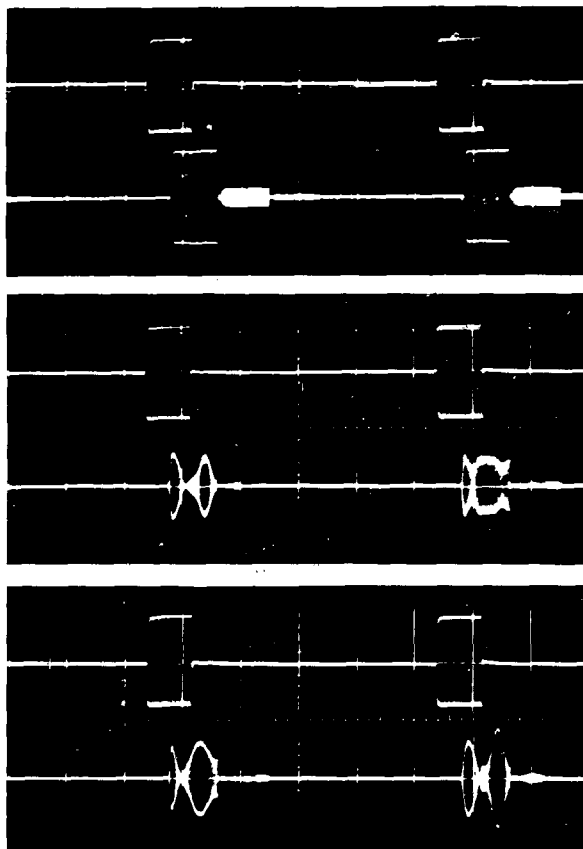


Fig. 3 Oscillograms showing transmitted and received sound pulses (upper and lower trace, respectively). First oscillogram obtained without flow, second and third ones with turbulent flow in the test duct (the same flow in both pictures). Sound frequency: 200 kcps; pulse length: 1.6 ms; pulse recurrence frequency: 100 cps

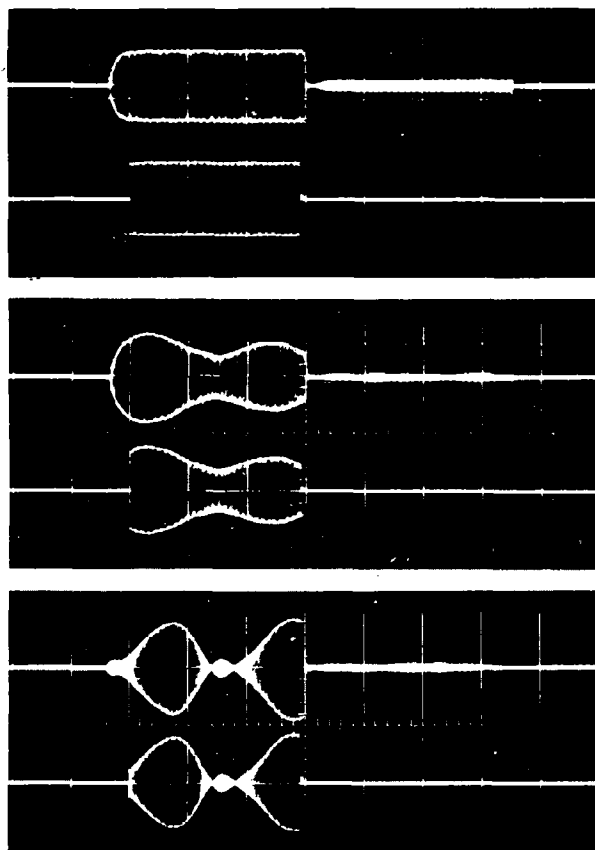


Fig.4 Examples of oscillograms, each one showing one directly received sound pulse, followed by reflections, and the portion selected for measurement (upper and lower trace, respectively). First oscillogram obtained without flow, second and third ones with turbulent flow in the test duct (the same flow in both pictures). Sound frequency: 200 kcps; pulse length: 1.6 ms; pulse recurrence frequency: 100 cps

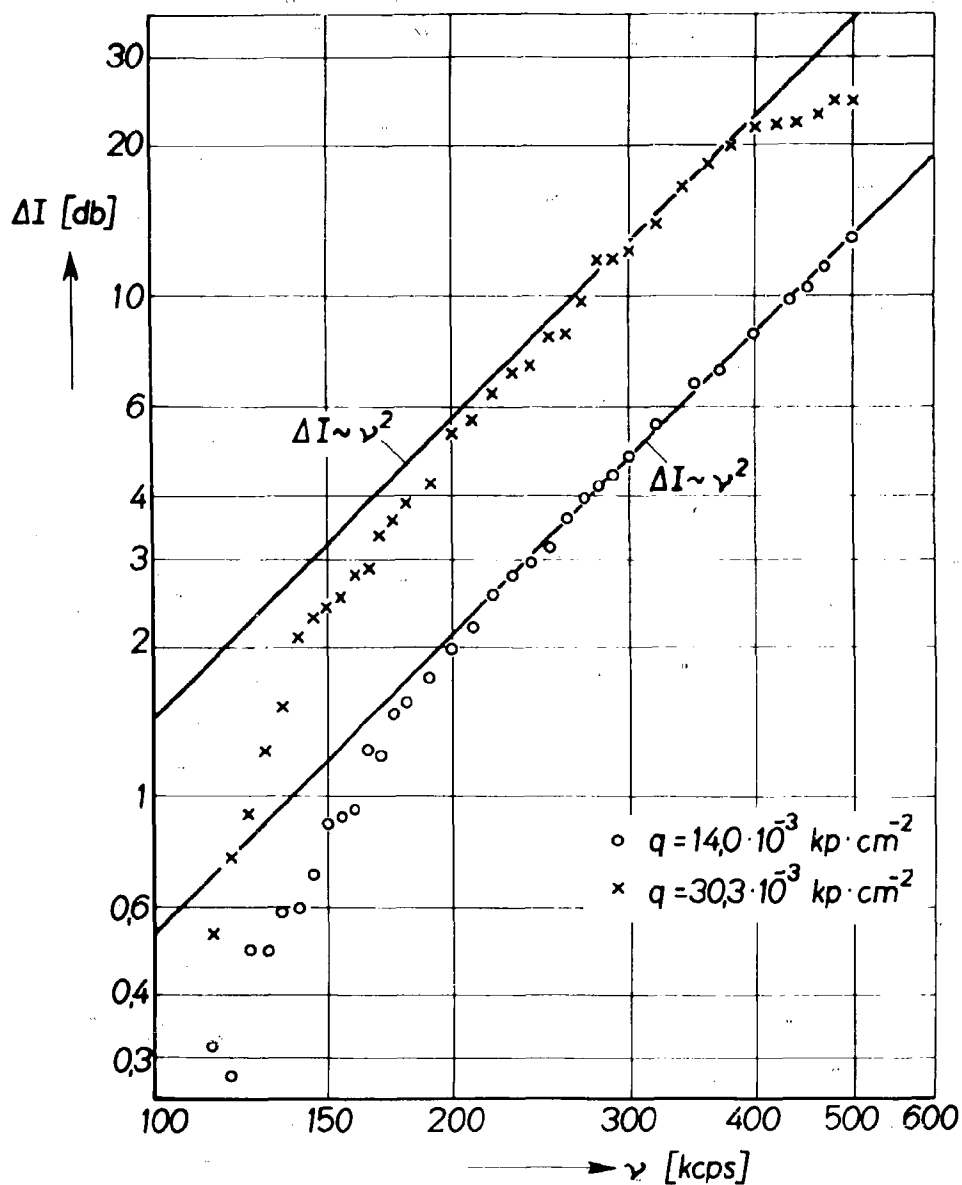


Fig. 5 Attenuation ΔI of sound vs. frequency of sound in the transition region between the asymptotic power laws $\Delta I \sim \nu^2$ and $\Delta I \sim \nu^5$. (The lines are the asymptotes in the ν^2 -region.)

Test conditions: total length of the sound path (\approx tunnel height) $h = 30.0$ cm; diameter of the rods $D = 0.10$ cm; grid mesh length $m = 0.50$ cm; distance grid - sound beam axis $d = 5.0$ cm; diameter of sound transmitter S_S - diameter of sound receiver $S_E = 1.30$ cm

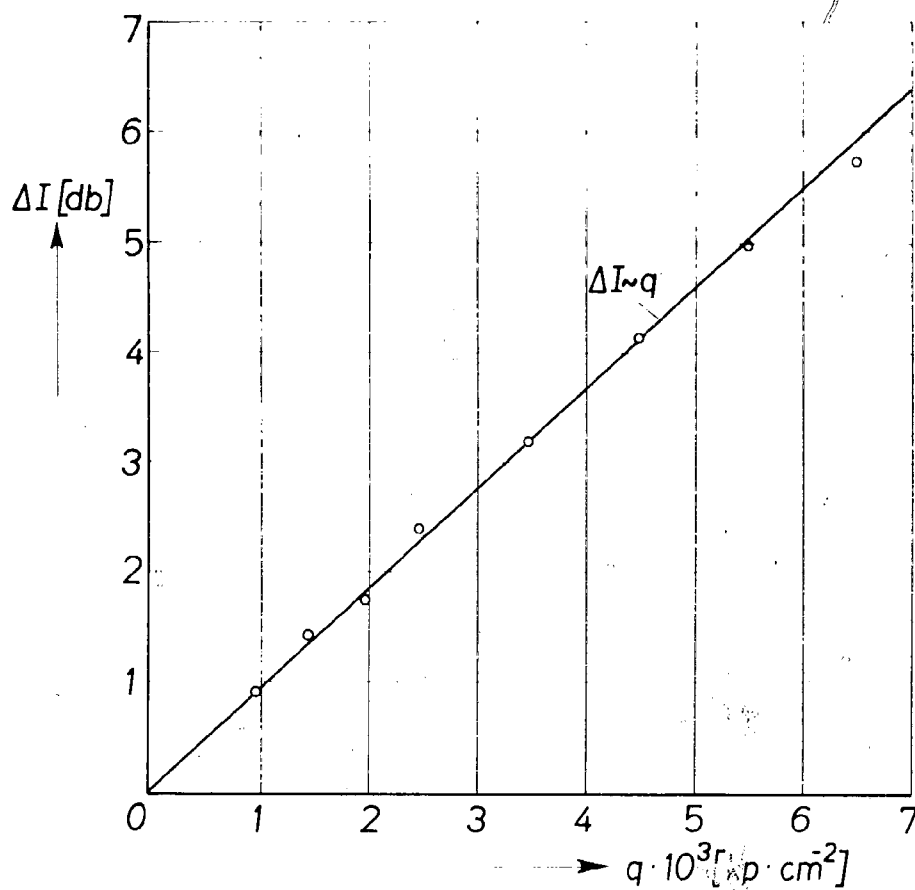


Fig. 6 Attenuation ΔI of sound vs. dynamic pressure q of the main flow.
 Test conditions: $h = 30.0 \text{ cm}$; $D = 1.00 \text{ cm}$; $m = 2.59 \text{ cm}$; $d = 21.0 \text{ cm}$;
 $\nu = 200 \text{ kcps}$; $S_S = S_E = 1.30 \text{ cm}$

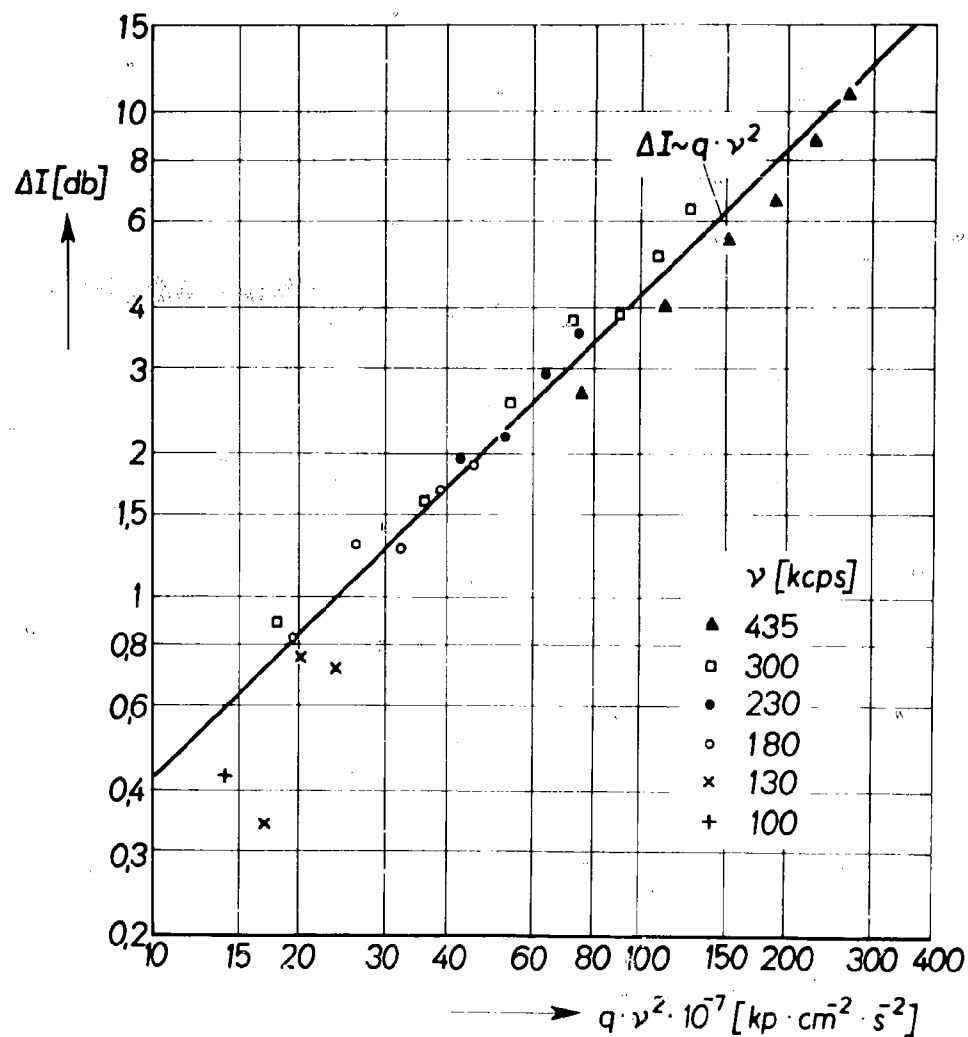


Fig. 7 Attenuation ΔI of sound vs. the product of the dynamic pressure q of the main flow and the square of the sound frequency ν .

Test conditions: $h = 30.0$ cm; $D = 0.15$ cm; $m = 2.50$ cm; $d = 5.0$ cm; $S_S = S_E = 1.30$ cm

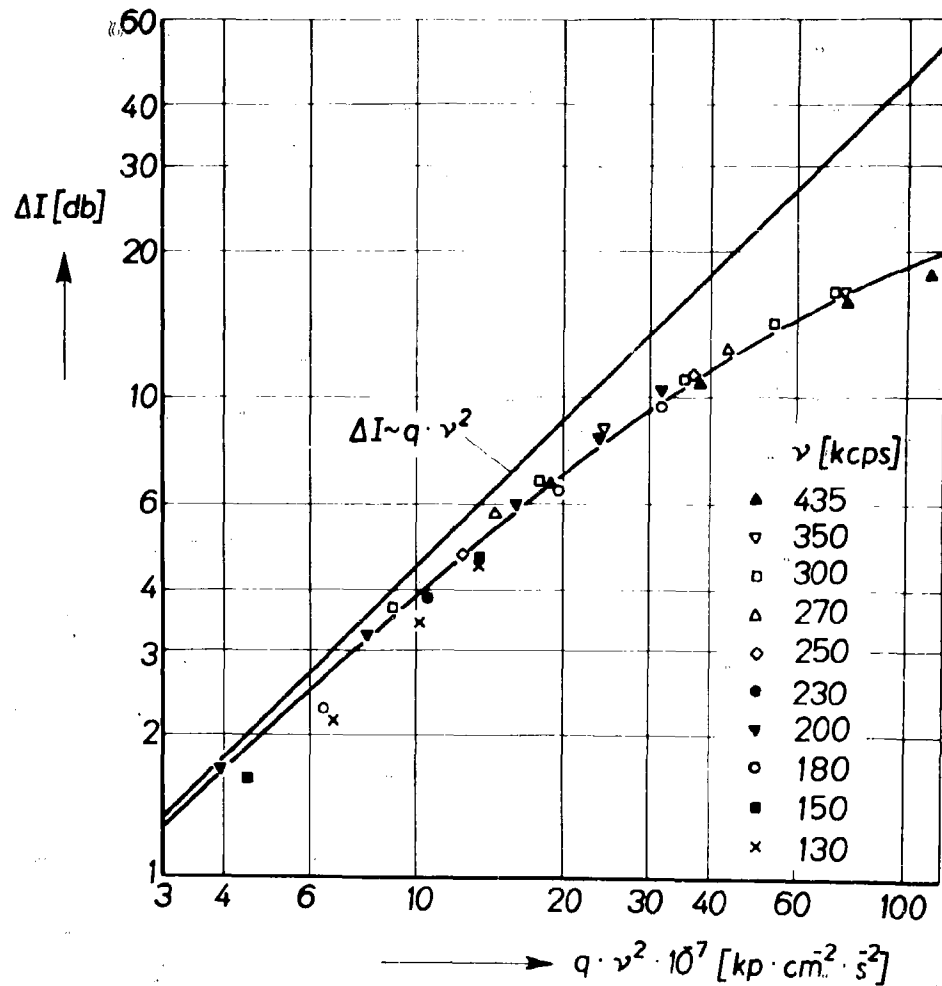


Fig. 8 Same as Figure 7 (test conditions changed).

Test conditions: $h = 30.0$ cm; $D = 1.00$ cm; $m = 2.50$ cm; $d = 20.0$ cm;
 $S_S = S_E = 1.30$ cm

The lower curve represents the equation

$$\Delta I = C_1 \cdot \frac{C_2 \cdot q \cdot \nu^2}{1 + C_2 \cdot q \cdot \nu^2}$$

with $C_1 = 32.2$ and $C_2 = 1.40 \cdot 10^{-9}$ cm² · s² · kp⁻¹; the straight line is its asymptote

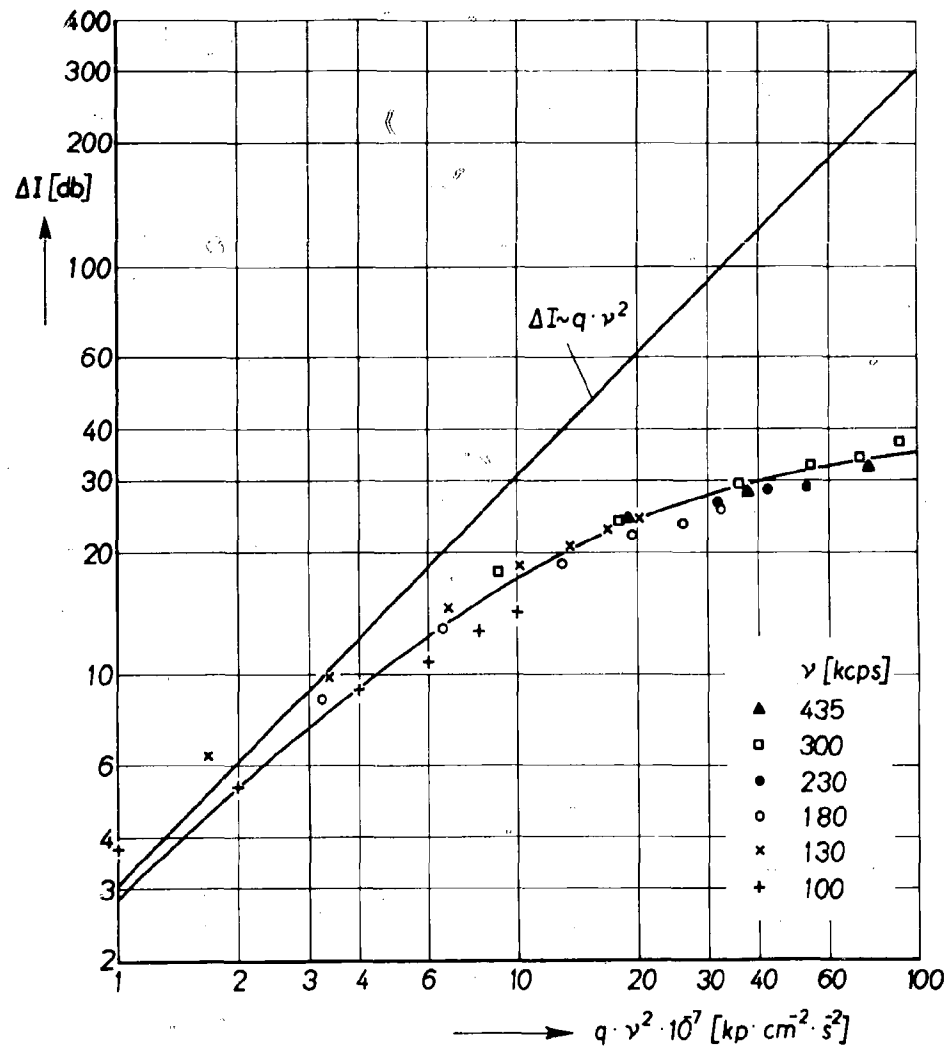


Fig.9 Same as Figure 7 (test conditions changed).

Test conditions: $h = 30.0$ cm; $D = 1.00$ cm; $m = 2.50$ cm; $d = 5.0$ cm;
 $S_S = S_E = 1.30$ cm

The lower curve represents the equation

$$\Delta I = C_1 \cdot \frac{C_2 \cdot q \cdot \nu^2}{1 + C_2 \cdot q \cdot \nu^2}$$

with $C_1 = 39.9$ and $C_2 = 7.63 \cdot 10^{-9} \text{ cm}^2 \cdot \text{s}^2 \cdot \text{kp}^{-1}$; the straight line is its asymptote

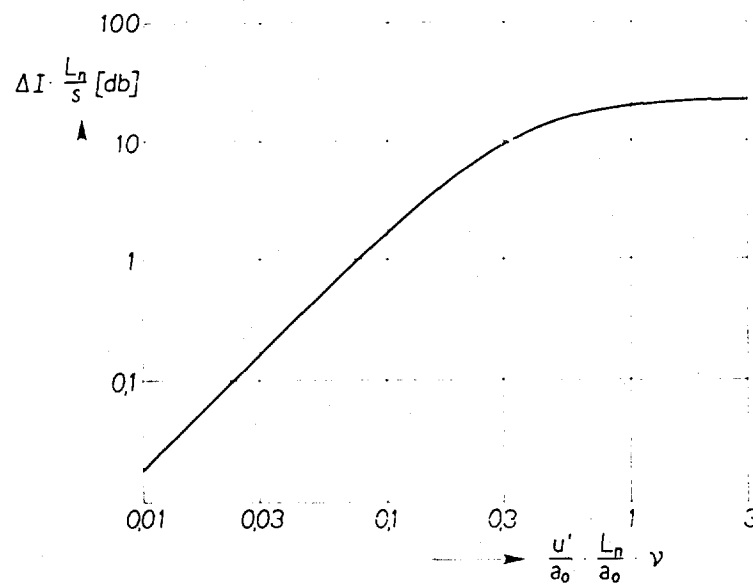


Fig. 10 Graphic representation of Equation (9) for the estimation of the scattering of sound by turbulence in the atmosphere

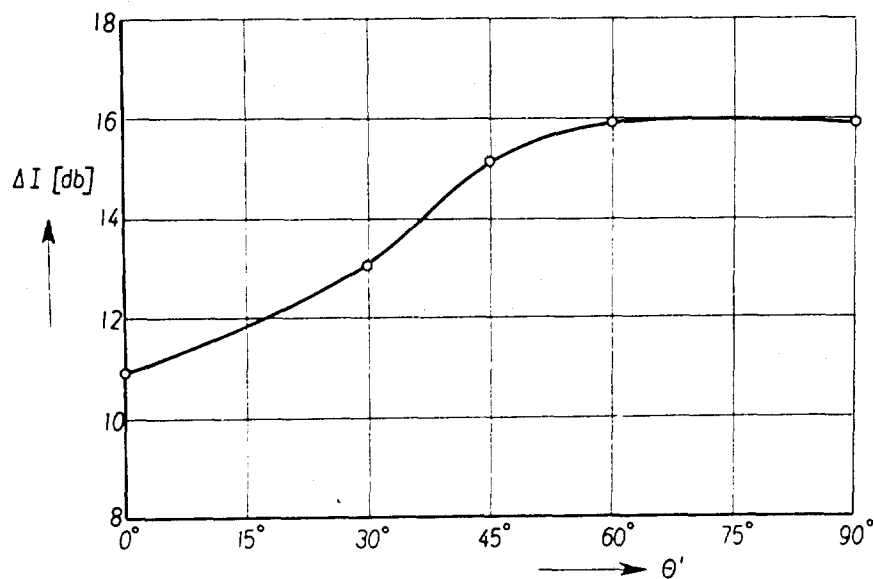


Fig. 11 Dependence of the turbulent sound attenuation ΔI on a predominant direction of the scattering vortices (θ' = angle between the rods of the turbulence grid and the direction of wave propagation).

Test conditions: $h = 30.0$ cm; $q = 4.2 \cdot 10^{-3}$ kp.cm $^{-2}$; $\nu = 220$ kcps; $D = 0.50$ cm;
 $m = 1.28$ cm; $d = 12.0$ cm; $S_S = S_E = 1.30$ cm

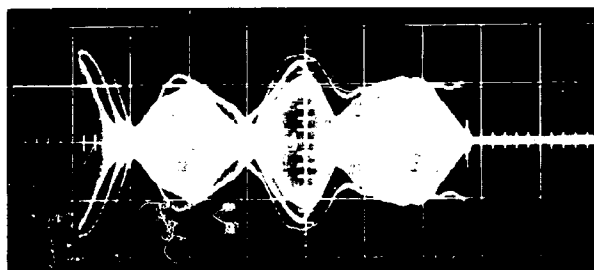


Fig. 12 Example of the regular amplitude modulation of ultrasound which has traversed the wake flow of a single bar. This pattern was obtained by superimposing three received sound pulses on the same picture.

Test conditions: $D = 0.60$ cm; $d = 3.0$ cm; $\nu = 350$ kcps

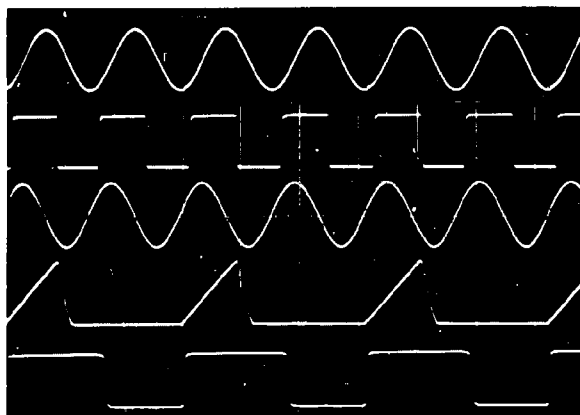


Fig. 13 Multiple oscillogram showing the relationships in time between some voltages which participate in the generation of phase-measuring sawtooth pulses

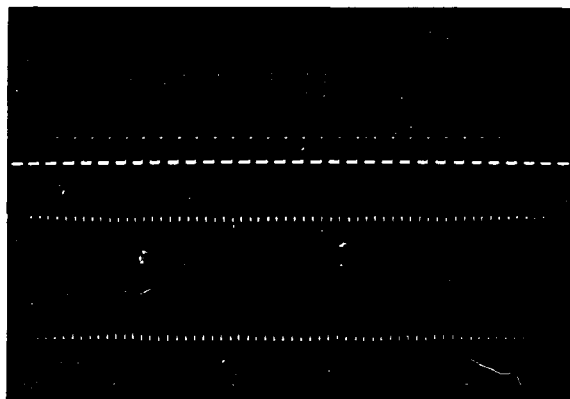


Fig.14 Double-beam oscillogram simultaneously showing phase- and amplitude-variations. It represents a time interval of 0.5 ms selected from within a received ultrasonic pulse in the case of laminar flow in the test duct (sound frequency: 129 keps)

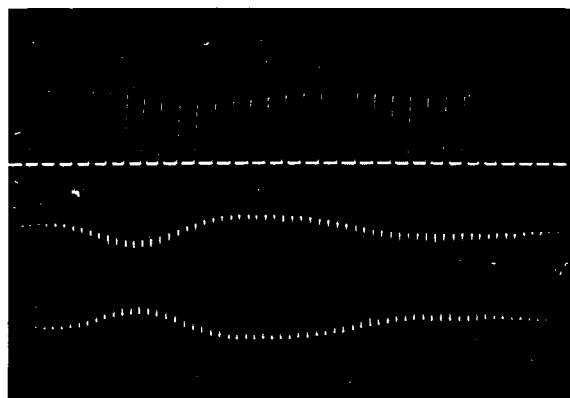


Fig.15 Same as Figure 14, but in the case of weak turbulent flow in the test duct

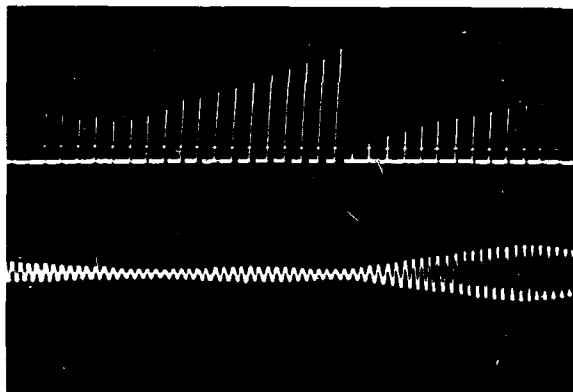


Fig. 16 Same as Figure 14, but in the case of strong turbulent flow in the test duct

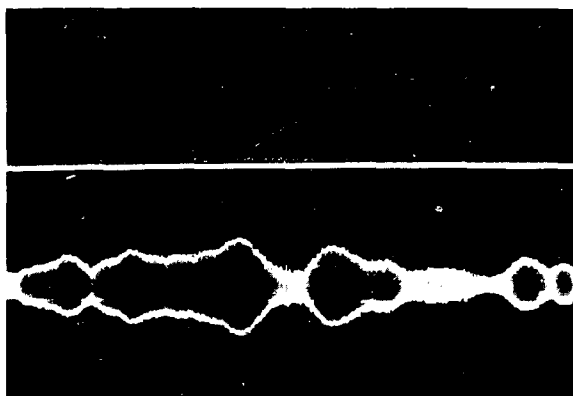


Fig. 17 Double-beam oscillogram simultaneously showing phase- and amplitude-variations. It represents a time interval of 3 ms selected from within a received ultrasonic pulse in the case of strong turbulent flow in the test duct (sound frequency: 300 kcps)

DISCUSSION

P.O.A.L. Davies

- (1) Are you aware of G.I. Taylor's report in 1913?
- (2) We made similar measurements but used continuous waves for $M'/M = 0.15L_x/\lambda = L_n^*$ and $L_n^* = 10 \rightarrow \nu = 10$ kc in a 5 by 5 ft tunnel by correlating the received with the transmitted waveforms. The bandwidth was spread from 8 to 12 kc for a 10 kc signal.

Author's reply

- (1) I am aware of G.I. Taylor's report in 1916, which was published in his Scientific Papers in 1960, as was referred to in my paper (1).
- (2) It is very interesting for me to hear about your experiments. We did also observe a certain spread of the bandwidth of the received sound signals, but we did not investigate this effect quantitatively.

G.M. Lilley

Do you think it is possible to use a similar method for looking at the attenuation of shock waves and the change in shock profile in their passage through turbulence? This problem has some current interest.

Author's reply

Yes, I think that a method of measurements similar to ours might be applicable for this purpose. One would have to replace our sound transmitter by a suitable shock tube and, perhaps, the receiving condenser microphone by a special pressure transducer which is fit for the reception of shock waves. Thank you for this suggestion, I will think it over further.

A. Powell

I wish to compliment Dr. Schmidt on the excellence of the experimental work. Are there any plans for observing the directional properties of the scattered sound? If Dr. Schmidt could do this with his usual accuracy, it may be possible, additionally, to detect the loss of total acoustic energy by the eddy viscosity (Reynolds stress) of the turbulence.

Author's reply

We do not plan to perform measurements of the directional properties of the scattered sound. The sound intensities to be measured would be lower than the intensity of the unscattered sound by one or even several orders of magnitude. I fear that the accuracy of the measurements of such low intensity sound waves would not meet the requirements for the detection of the energy loss due to turbulent eddy viscosity.

DISTRIBUTION

Copies of AGARD publications may be obtained in the various countries at the addresses given below.

On peut se procurer des exemplaires des publications de l'AGARD aux adresses suivantes.

BELGIUM BELGIQUE	Centre National d'Etudes et de Recherches Aéronautiques 11, rue d'Egmont, Bruxelles
CANADA	Director of Scientific Information Service Defense Research Board Department of National Defense 'A' Building, Ottawa, Ontario
DENMARK DANEMARK	Military Research Board Defense Staff Kastellet, Copenhagen Ø
FRANCE	O.N.E.R.A. (Direction) 25, Avenue de la Division Leclerc Châtillon-sous-Bagneux (Seine)
GERMANY ALLEMAGNE	Zentralstelle für Luftfahrt- dokumentation und -information München 27, Maria-Theresia Str. 21 Attn: Dr. H.J. Rautenberg
GREECE GRECE	Greek National Defense General Staff B. MEO Athens
ICELAND ISLANDE	Director of Aviation c/o Flugrad Reykjavik
ITALY ITALIE	Ufficio del Generale Ispettore del Genio Aeronautico Ministero Difesa Aeronautica Roma
LUXEMBURG LUXEMBOURG	Obtainable through Belgium
NETHERLANDS PAYS BAS	Netherlands Delegation to AGARD Michiel de Ruyterweg 10 Delft

NORWAY
NORVEGE

Mr. O. Blichner
Norwegian Defence Research Establishment
Kjeller per Lilleström

PORTUGAL

Col. J.A. de Almeida Viama
(Delegado Nacional do 'AGARD')
Direcção do Serviço de Material da F.A.
Rua da Escola Politecnica, 42
Lisboa

TURKEY
TURQUIE

Ministry of National Defence
Ankara
Attn. AGARD National Delegate

UNITED KINGDOM
ROYAUME UNI

Ministry of Aviation
T.I.L., Room 009A
First Avenue House
High Holborn
London W.C.1

UNITED STATES
ETATS UNIS

National Aeronautics and Space Administration
(NASA)
1520 H Street, N.W.
Washington 25, D.C.



*Printed by Technical Editing and Reproduction Ltd
Harford House, 7-9 Charlotte St. London. W. 1.*

This document
**Reproduced From
Best Available Copy**

<p>AGARD Report 461 North Atlantic Treaty Organization, Advisory Group for Aeronautical Research and Development RECENT EXPERIMENTAL INVESTIGATIONS OF THE SCATTER- ING OF SOUND BY TURBULENCE Dieter W. Schmidt 1963 23 pp., incl. 7 refs., 17 figs. & discussion</p> <p>Experimental investigations of the scattering of sound by turbulence were performed in a wind tunnel. Recent theoretical predictions concerning the sound attenuation are well confirmed and partly extended by the measurements. In the range of the parameters which is of interest for practical applications the most important results obtained are the propor-</p> <p>P. T. O.</p>	<p>534.26:532.517.4 1c5:3b2f</p>	<p>AGARD Report 461 North Atlantic Treaty Organization, Advisory Group for Aeronautical Research and Development RECENT EXPERIMENTAL INVESTIGATIONS OF THE SCATTER- ING OF SOUND BY TURBULENCE Dieter W. Schmidt 1963 23 pp., incl. 7 refs., 17 figs. & discussion</p> <p>Experimental investigations of the scattering of sound by turbulence were performed in a wind tunnel. Recent theoretical predictions concerning the sound attenuation are well confirmed and partly extended by the measurements. In the range of the parameters which is of interest for practical applications the most important results obtained are the propor-</p> <p>P. T. O.</p>	<p>534.26:532.517.4 1c5:3b2f</p>
<p>AGARD Report 461 North Atlantic Treaty Organization, Advisory Group for Aeronautical Research and Development RECENT EXPERIMENTAL INVESTIGATIONS OF THE SCATTER- ING OF SOUND BY TURBULENCE Dieter W. Schmidt 1963 23 pp., incl. 7 refs., 17 figs. & discussion</p> <p>Experimental investigations of the scattering of sound by turbulence were performed in a wind tunnel. Recent theoretical predictions concerning the sound attenuation are well confirmed and partly extended by the measurements. In the range of the parameters which is of interest for practical applications the most important results obtained are the propor-</p> <p>P. T. O.</p>	<p>534.26:532.517.4 1c5:3b2f</p>	<p>AGARD Report 461 North Atlantic Treaty Organization, Advisory Group for Aeronautical Research and Development RECENT EXPERIMENTAL INVESTIGATIONS OF THE SCATTER- ING OF SOUND BY TURBULENCE Dieter W. Schmidt 1963 23 pp., incl. 7 refs., 17 figs. & discussion</p> <p>Experimental investigations of the scattering of sound by turbulence were performed in a wind tunnel. Recent theoretical predictions concerning the sound attenuation are well confirmed and partly extended by the measurements. In the range of the parameters which is of interest for practical applications the most important results obtained are the propor-</p> <p>P. T. O.</p>	<p>534.26:532.517.4 1c5:3b2f</p>

tionality of the sound attenuation to the square of the sound frequency and of the square of the turbulent Mach number. A formula is derived from which the turbulent attenuation of directed sound (such as aircraft noise in the free atmosphere) can be calculated. A method for measuring large phase variations is described in preliminary form; it will be used to investigate the influence of turbulent scattering on the phase angle of the sound waves.

This Report is one in the Series 448-469 inclusive, presenting papers, with discussions, given at the AGARD Specialists' Meeting on 'The Mechanism of Noise Generation in Turbulent Flow' at the Training Center for Experimental Aerodynamics, Rhode-Saint-Genèse, Belgium, 1-5 April 1963, sponsored by the AGARD Fluid Dynamics Panel.

tionality of the sound attenuation to the square of the sound frequency and to the square of the turbulent Mach number. A formula is derived from which the turbulent attenuation of directed sound (such as aircraft noise in the free atmosphere) can be calculated. A method for measuring large phase variations is described in preliminary form; it will be used to investigate the influence of turbulent scattering on the phase angle of the sound waves.

This Report is one in the Series 448-469 inclusive, presenting papers, with discussions, given at the AGARD Specialists' Meeting on 'The Mechanism of Noise Generation in Turbulent Flow' at the Training Center for Experimental Aerodynamics, Rhode-Saint-Genèse, Belgium, 1-5 April 1963, sponsored by the AGARD Fluid Dynamics Panel.

tionality of the sound attenuation to the square of the sound frequency and to the square of the turbulent Mach number. A formula is derived from which the turbulent attenuation of directed sound (such as aircraft noise in the free atmosphere) can be calculated. A method for measuring large phase variations is described in preliminary form; it will be used to investigate the influence of turbulent scattering on the phase angle of sound waves.

This Report is one in the Series 448-469 inclusive, presenting papers, with discussions, given at the AGARD Specialists' Meeting on 'The Mechanism of Noise Generation in Turbulent Flow' at the Training Center for Experimental Aerodynamics, Rhode-Saint-Genèse, Belgium, 1-5 April 1963, sponsored by the AGARD Fluid Dynamics Panel.

tionality of the sound attenuation to the square of the sound frequency and to the square of the turbulent Mach number. A formula is derived from which the turbulent attenuation of directed sound (such as aircraft noise in the free atmosphere) can be calculated. A method for measuring large phase variations is described in preliminary form; it will be used to investigate the influence of turbulent scattering on the phase angle of the sound waves.

This Report is one in the Series 448-469 inclusive, presenting papers, with discussions, given at the AGARD Specialists' Meeting on 'The Mechanism of Noise Generation in Turbulent Flow' at the Training Center for Experimental Aerodynamics, Rhode-Saint-Genèse, Belgium, 1-5 April 1963, sponsored by the AGARD Fluid Dynamics Panel.